Structural and temperature dependence of the optical and magneto-optical properties of the Heusler Ni_2MnGa alloy

Y. V. Kudryavtsev
Institute of Metal Physics, National Academy of Sciences of Ukraine, 36 Vernadsky str, 03142, Kiev-142, Ukraine

Y. P. Lee
Quantum Photonic Science Research Center and Department of Physics, Hanyang University, 17 Haengdang-Dong, Sungdong-Ku, Seoul, 133-791 Korea

J. Y. Rhee
Department of Physics, Hoseo University, Asan, Choongnam, 336-795 Korea

(Received 13 April 2002; published 26 September 2002)

The influence of martensitic and magnetic phase transformations on the optical and magneto-optical (MO) properties of polycrystalline Ni_2MnGa alloy samples, in bulk and thin films, has been investigated. The parameters of charge carriers (plasma and relaxation frequencies) were determined for all the aforementioned states. By the analogy with the band structure and optical properties of the Ni_2MnSn alloy the nature of interband absorption peaks in the optical-conductivity (OC) spectrum of Ni_2MnGa alloy, located at 1.78 and 3.40 eV, is discussed. It was shown that a cooling of substrate with liquid nitrogen during the film deposition leads to the formation of an amorphous phase in the Ni_2MnGa alloy, which, unlike the bulk sample, is not ferromagnetically ordered at 293 K. An annealing of the amorphous film at 680 K for 60 min restores its crystallinity and also the ferromagnetic order. The off-diagonal components of the dielectric function (DF) for the cubic phase of the Ni_2MnGa alloy were determined. Like in the interband OC spectrum, the absorptive part of the off-diagonal components of the DF exhibits a two-peak structure, in which the low-energy peak is located at the same energy as in the OC spectrum. Both optical and MO properties of the Ni_2MnGa alloy show a noticeable structural dependence; the more intense the peaks, the better the crystallinity of the sample. It was shown that the value of the MO response for Ni_2MnGa alloy was strongly influenced by the optical properties, indicating a close connection between them.

DOI: 10.1103/PhysRevB.66.115114 PACS number(s): 78.20.Ci, 78.20.Ls, 78.66.Bz

I. INTRODUCTION

The experimental finding of a huge polar magneto-optical (MO) Kerr effect in a ferromagnetic semi-Heusler PtMnSb alloy by van Engen[1] has inspired a great deal of interest in the study of the electronic structure, and the MO and optical properties of similar compounds. The semi-Heusler phases are cubic ternary compounds, crystallized in a $C1_b$ structure, and have a formula of XYZ, where X and $Y$are transition metals and Z is an sp element. They are derived from the true Heusler phases of formula X_2YZ, in an $L2_1$ crystalline structure, by removing one X atom leaving a vacant site. The huge MO effect of these alloys is usually explained by the specific electronic structure. These compounds are thought to be metallic for one spin direction while they show semiconducting properties for the opposite spin direction. This phenomenon is called half-metallic ferromagnetism. That is why the MO and optical properties as well as the electronic structures of semi-Heusler[2–14] and true Heusler[15–21] alloys have been intensively studied experimentally and theoretically since the early 1980s.

Among ferromagnetic true Heusler alloys the Ni_2MnGa alloy has additionally attracted a considerable interest due to the shape-memory effect, the superelasticity, and a large magnetocaloric effect.[22–24] The stoichiometric Ni_2MnGa alloy exhibits the martensitic transformation from the tetragonal to the cubic phase at 202 K and has a Curie temperature of 376 K. However, in spite of the great interest in this alloy its electronic structure has been insufficiently investigated. In contrast to other ferromagnetic Heusler alloys, the dielectric function (DF) of the Ni_2MnGa alloy, as far as we know, was not studied yet experimentally or theoretically.

The electronic structures of the Ni_2MnGa alloy in the cubic and the tetragonal phases, and also in the cubic ferromagnetic and paramagnetic states were calculated by Pugaczowa-Michalska[25] and by Velikohatnyj and Naumov.[26] According to these results the Ni_2MnGa alloy cannot be considered a pure half-metallic compound, since the density of states (DOS) at the Fermi level (E_F) is composed of both spin components. However, E_F for the ferromagnetic cubic phase is located in a valley between two intense peaks of the minority-spin subbands, created by the occupied $3d$ states of Ni and the empty $4d$ states of Ga. For the majority-spin subband, E_F also lies in the minimum between two intense peaks, formed by the occupied $3d$ states of Mn and the empty $4d$ states of Ga.[26] We should be very cautious regarding this matter since the unoccupied Ga $4d$ bands are missing in Ref. 25. Because nearly all the $3d$ states of Ni are occupied (in contrast to the $3d$ states of Mn), the main contribution to the total magnetic moment of the alloy ($4.10\mu_B$) comes from the Mn atoms ($3.49\mu_B$) while the magnetic moments of the Ni and Ga atoms are rather small (i.e., 0.33 and

$-0.05\mu_B$, respectively). The transition to the paramagnetic cubic state leads to drastic changes in the electronic structure of the alloy. The splitting of Mn $3d$ states disappears and the DOS at the Fermi level increases by five times.[26] In contrast to the case of ferromagnetic-paramagnetic transformation, the DOS for the tetragonal phase differs insignificantly from that for the cubic one.[25]

It is known that for Mn-containing Heusler alloys the exchange interaction is indirect, involving polarization of the conduction electrons. Therefore, any change in the chemical or atomic order may influence directly the magnetic behavior of the alloy. On the other hand, it is also well known that fundamentally the MO Kerr effect is caused by the simultaneous occurrence of spin polarization and spin-orbit coupling in a magnetic solid. Therefore, the dependence of the MO properties of the Ni_2MnGa alloy on the chemical or atomic order can be expected. The MO properties of a medium [i.e., the off-diagonal components of the DF ($\tilde{\varepsilon}$); $\tilde{\varepsilon}_{xy}=-\tilde{\varepsilon}_{yx}=i\tilde{\varepsilon}'$ where $\tilde{\varepsilon}'=\varepsilon_1'-i\varepsilon_2'$] cannot be determined without knowledge of its optical properties (i.e., the diagonal components of the DF; $\tilde{\varepsilon}_{xx}=\tilde{\varepsilon}_{yy}=\tilde{\varepsilon}_{zz}=\varepsilon=\varepsilon_1-i\varepsilon_2$, where $\varepsilon_1=n^2-k^2$ and $\varepsilon_2=2nk$. n and k are the refractive index and the extinction coefficient, respectively). Furthermore, as was shown by Halilov and Kulatov,[5] 100% spin polarization at E_F, a large magnetic moment and a significant spin-orbit interaction do not always guarantee a large MO effect. They showed that plasma resonance or peculiarities in the optical properties may play a more decisive role for the MO effect of Heusler alloys.

The purpose of this work is to study experimentally the influence of the structural disordering as well as the martensitic and ferromagnetic-paramagnetic transitions on the optical and MO properties of the Ni_2MnGa alloy. In order to study the structural dependence of the aforementioned properties more comprehensively, several alloy-film samples were additionally investigated. This paper is organized as follows; Sec. II contains a description of the sample preparation and the experimental details, the results are analyzed and discussed in Sec. III which is again divided into three subsections, and Sec. IV summarizes and concludes the paper.

II. EXPERIMENTAL PROCEDURE

Bulk Ni_2MnGa alloy was prepared by melting Ni, Mn, and Ga pieces of 99.99% purity together in an arc furnace with a water-cooled Cu hearth. In order to obtain the volume homogeneity the ingot was remelted twice, annealed at 1300 K for 6 h, and then slowly cooled. Any weight loss after melting and heat treatment was not observed. X-ray fluorescence analysis revealed an alloy composition of $Ni_{0.493}Mn_{0.247}Ga_{0.260}$.

For the optical and MO measurements a slab of about $15\times8\times2$ mm^3 was cut from the ingot using a spark-erosion technique and then polished mechanically with diamond powders. The final stage of polishing was carried out using Cr_2O_3 powders. After this the sample surface was cleaned with acetone and ethanol using an ultrasonic cleaner. To remove the surface contamination introduced by the mechanical treatment, the sample was annealed in a high vacuum at 760 K for 3 h. After such a treatment the surface was further electropolished at room temperature (RT) in a 1:2 mixture of nitric acid and ethanol and at a current density of about 10 mA/cm^2. Then, the surface was cleaned again and the sample was put into a vacuum chamber for the optical measurements. The optical properties of the bulk Ni_2MnGa alloy were studied for the as-polished sample, after annealing and also after electropolishing.

TABLE I. Parameters of the investigated Ni_2MnGa alloy films. T and t are substrate temperature during the deposition and film thickness, respectively.

Film sample number	T (K)	Heat treatment	t (nm)
1	720		118
2	150		79
3	150		186
4	150	680 K/60 min	256

Ni_2MnGa alloy films of 10×30 mm^2 were prepared by flash evaporation of the crushed alloy powders of $80-100\mu$m in diameter simultaneously onto glass and NaCl substrates in a vacuum better than 5×10^{-5} Pa. The alloy powders were prepared from the same ingot of the bulk Ni_2MnGa alloy. The most ordered (for our case) state of the Ni_2MnGa alloy films was achieved by the deposition onto substrates heated up to 720 K (sample 1). In order to obtain a substantially disordered state in the film, a vapor-quenching-deposition technique was employed, where a chaos of the gas phase is condensed onto substrates cooled down to 150 K by liquid nitrogen (samples 2–4). One of the latter films (i.e., deposited at 150 K) was annealed *in situ* at 680 K for 60 min after the optical measurements and its optical and MO properties were measured again. The parameters of the prepared Ni_2MnGa alloy films are shown in Table I.

The structural characterization of the bulk and film Ni_2MnGa alloy samples has been performed using x-ray diffraction (XRD) with Cu K_α radiation. A transmission-electron microscopy (TEM) study was additionally carried out for the films deposited onto NaCl substrates.

The optical properties of Ni_2MnGa samples were measured using a rotating-analyzer spectroscopic ellipsometer below and above the martensitic transformation temperature and also below and above the Curie temperature, i.e., at 78, 293, 408, and 460 K in a spectral range of 310–2500 nm (4.0–0.5 eV) at a fixed incidence angle of 73°. The MO properties (equatorial Kerr effect: EKE, δ_p) were investigated at RT by the dynamical method using *p*-plane polarized light at two angles of incidence (66° and 75°) in a spectral range of 310–1100 nm (4.0–1.05 eV). The other details of the optical and MO measurements can be found elsewhere.[27]

The resistivity measurements were carried out using the four-probe technique in a temperature range 5–395 K for the bulk sample of about $15\times2\times0.5$ mm^3, which was cut from the same ingot by spark erosion, and also in the 5–300 K

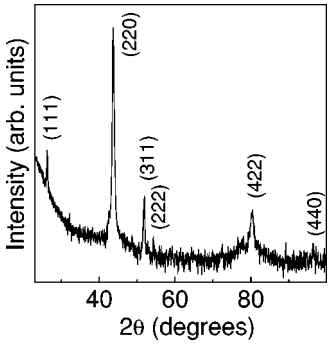

FIG. 1. X-ray-diffraction pattern for the bulk Ni_2MnGa alloy.

region for the crystalline Ni_2MnGa alloy film (sample No. 1). Temperature dependence of the magnetic properties of the bulk Ni_2MnGa alloy was investigated by measuring the magnetic susceptibility $\chi(T)$ using a superconducting quantum interference device in an external field of 100 G and in the 5–395 K temperature range. The magnetic properties of Ni_2MnGa alloy films were studied at RT with a vibrating sample magnetometer (VSM) for the in-plane geometry.

III. RESULTS AND DISCUSSION

A. Structural, magnetic, and transport properties

The structural homogeneity of the investigated bulk and film samples was proven to be single phase, and only diffraction relevant to the $L2_1$ phase is observed on the XRD spectra for the bulk and film Ni_2MnGa alloy (see Fig. 1).

The lattice parameters for the cubic phase were determined to be 0.5852 and 0.5836 nm for bulk and crystalline films (sample No. 1), respectively. Additionally, the TEM patterns (not shown) for the film deposited onto a substrate at 720 K exhibit only spots typical for the single-crystalline $L2_1$ structure (for the microdiffraction) and show a mean grain size of about 40–50 nm. A decrease in the substrate temperature down to 150 K leads to formation of a considerably disordered polycrystalline- (or more probably amorphous) alloy film with a few smeared halos on the diffraction pattern and a mean grain size, if any, less than the resolution limit of TEM. An annealing of such an amorphous film at 680 K for 60 min causes recovery of the crystalline structure and appearance of the diffraction rings typical for the $L2_1$ phase. However, this film has a slightly smaller mean grain size ($\sim$30 nm) than that for the films deposited onto substrates at 720 K.

The magnetic and transport properties of Ni_2MnGa alloys near the stoichiometric composition have been widely investigated, and such properties of our samples can give us useful information concerning their homogeneity, composition, and crystalline quality. Figure 2 presents the results of the temperature dependencies of magnetic susceptibility and resistivity for the bulk and crystalline-film (obtained at 720 K) Ni_2 MnGa alloy samples. It is seen that near 224 K the $\chi(T)$ increases abruptly and also that the temperature dependence of resistivity for the bulk alloy exhibits a noticeable slope change at the same temperature.

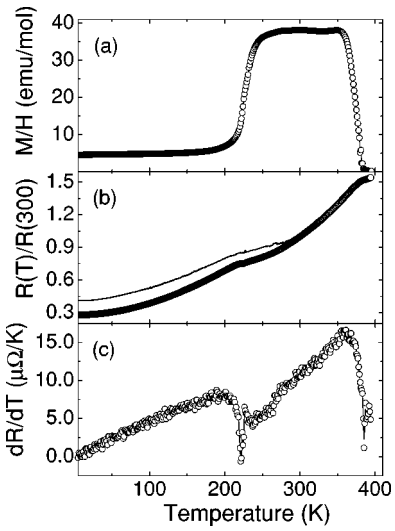

FIG. 2. Temperature dependence of the (a) magnetic susceptibility χ, and (b) resistivity (normalized with respect to that at 300 K) of the bulk (open circles) and crystalline-film (line, sample No. 1) Ni_2MnGa alloy. (c) Derivative of the temperature dependence of resistivity.

The origin of the observed phenomena can be confidently related to the martensitic transformation, which takes place at 224 K in our bulk alloy. A further increase in temperature leads to an abrupt fall of χ down to nearly zero at 379 K, which indicates a transition of the alloy into the paramagnetic state. This transition is also accompanied by noticeable anomalies in the $R(T)$ and $\partial R/\partial T$ plots [see Figs. 2(b) and 2(c)]. The $R(T)$ dependence for the crystalline Ni_2MnGa alloy film (sample 1) also shows the peculiarity exactly at the same temperature as for the bulk sample, however, the $R(300\ \mathrm{K})/R(5\ \mathrm{K})$ ratio for the film is somewhat smaller than that for the bulk sample. Both facts may support the exact reproduction of bulk alloy composition in the film, however, the crystallinity of film sample No. 1, our best crystalline-alloy film, is worse than that of the bulk alloy.

The temperature of martensitic transformation, $T_m = 224$ K, and the Curie temperature, $T_C = 379$ K, observed experimentally for our samples, are rather close to the known literature results for Ni_2MnGa alloys near the stoichiometric composition. Indeed, T_C for the exactly stoichiometric Ni_2MnGa alloy is reported to be 376 K (Refs. 28 and 29) or 382 K.[30] T_m measured on cooling for the exactly stoichiometric Ni_2MnGa alloy is known to be 202 K.[28,29] Some disagreement in T_m between our samples and the literature results can be explained by a thermal hysteresis of the martensitic transformation and/or a slight deviation in the alloy composition from the exact stoichiometry, as shown by x-ray fluorescence.

B. Optical properties of the alloy

The results of optical study at 293 K for the bulk Ni_2MnGa alloy sample are shown in Fig. 3. It is seen that the measured optical properties of the Ni_2MnGa alloy are rather sensitive to the quality of the sample surface. The optical-

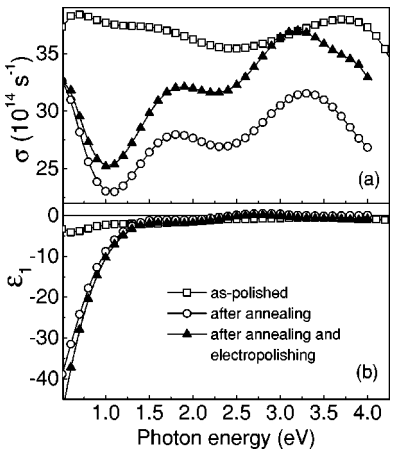

FIG. 3. (a) Optical conductivity and (b) ε_1 spectra at 293 K for the as-polished, annealed, and electropolished bulk Ni_2MnGa alloy.

conductivity (OC, σ) spectrum for the as-polished bulk sample is nearly structureless; weak and broad features at 1.5 and 3.9 eV are observed, and the absolute value of ε_1 in the near-infrared (NIR) region is relatively small. A heat treatment of the as-polished sample leads to a noticeable improvement of the crystalline structure in the surface layer destroyed by mechanical polishing and spark-erosion treatment. Indeed, after such a treatment the pronounced interband absorption peaks near 1.7 and 3.2 eV are seen in the OC spectrum of the alloy, and the absolute value of ε_1 in the NIR region is significantly increased, indicating an enhancement of the free-electron-like absorption. A certain decrease of OC as a whole is also observed. A possible reason for this shift in $\sigma(\omega)$ will be discussed further. However, it is seen that the annealing only is not enough for the complete elimination of structural defects introduced by spark erosion and mechanical polishing of the sample. Electropolishing makes the surface more perfect since the procedure enhances the magnitude of OC and increases the absolute value of ε_1 in the NIR region. Nearly the same regularity in the structural dependence of optical properties is also obtained for the investigated Ni_2MnGa alloy films. The OC spectrum at 293 K for the amorphous Ni_2MnGa alloy film exhibits weak features on a flat plateau (see Fig. 4).

An annealing of the amorphous film, which restores the crystalline structure, makes the interband absorption peaks at $\sim$ 1.7 and 3.2 eV in the OC spectrum more pronounced, decreases the OC value as a whole, and increases the absolute value of ε_1 in the NIR region. However, the intensities of interband absorption peaks in the OC spectrum and the absolute value of ε_1 in the NIR region for sample 1, which, according to the results of the TEM study, has a better crystallinity than film sample 4, turn out to be even larger than those for the annealed sample 4. Thus, we can conclude that both bulk and film Ni_2MnGa alloy samples follow a common regularity in the dependence of optical properties on the sample crystallinity.

The influence of the martensitic and magnetic transitions on the optical properties of Ni_2MnGa alloy was studied for the bulk sample whose surface was prepared by electropolishing (see Fig. 5). It is seen that for all the temperatures and

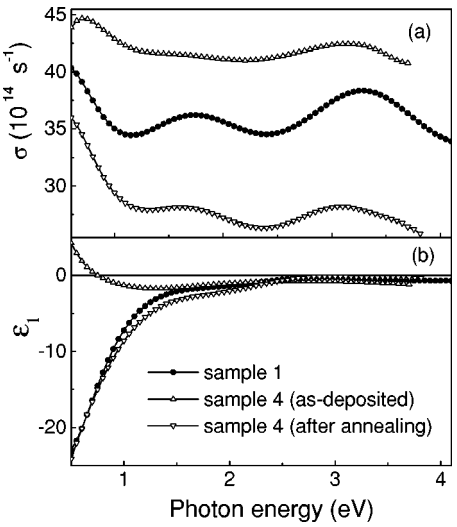

FIG. 4. (a) Optical conductivity and (b) ε_1 spectra at 293 K for the Ni_2MnGa alloy film deposited onto a substrate cooled by liquid nitrogen, for the same film but after an annealing at 680 K/60 min, and for the film deposited at 720 K.

hence for all the states the OC spectra exhibit two absorption peaks at $\sim$1.7 and 3.2 eV, and the ε_1 spectra present anomalous dispersion nearly at the same energies [see the inset of Fig. 5(a)]. At the same time, below $\hbar\omega < 1$ eV the ε_1 and σ spectra at all the investigated temperatures look Drude-like. A more definite conclusion on the character of optical absorption in the NIR region can be made by observing the $\omega\varepsilon_2$ vs ε_1 plot, the so-called Argand diagram, whose linear part is interpreted as the free-electron absorption. An entirely

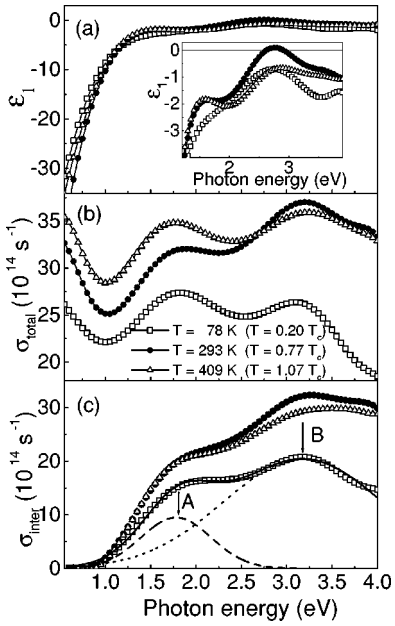

FIG. 5. (a) ε_1, (b) total OC, and (c) interband OC spectra for the electropolished bulk Ni_2MnGa alloy, measured at 78 K, 293 K, and 409 K. Inset in (a) presents an expanded view of the ε_1 spectra in a high-energy region. Dashed and dotted lines in (c) show interband contributions to the fitted interband OC spectrum (solid line) obtained for $T = 78$ K by using the multiple-peak analysis.

TABLE II. Plasma, Ω_P, and relaxation, γ, frequencies as well as the parameters of low-energy (A) and high-energy (B) interband absorption peaks in the OC spectra for the electropolished bulk Ni_2MnGa alloy, obtained at different temperatures. $\hbar\omega_0, \Delta\hbar\omega$, and I are the location, full width at half maximum, and intensity, respectively, for the interband absorption peaks.

Temperature (K)	Ω_P^2 (10^{30} s^{-2})	γ (10^{14} s^{-1})	$\hbar\omega_0^A$ (eV)	$\hbar\omega_0^B$ (eV)	$\Delta\hbar\omega^A$ (eV)	$\Delta\hbar\omega^B$ (eV)	I_A	I_B
78	5.83	2.32	1.78	3.19	0.83	1.70	10.1	43.6
293	8.69	3.14	1.78	3.40	0.77	2.06	10.0	85.6
409	12.33	3.97	1.78	3.45	0.79	2.06	11.4	79.9

linear region in the diagram was found for all the temperatures (not shown here), indicating the predominance of free-electron absorption below a photon energy of 1 eV. With this evidence that the free-electron or Drude absorption is dominant in the NIR region of spectra, the plasma frequency, Ω_P, and the effective relaxation frequency of free charge carriers, γ, were determined using a linear-regression analysis on the diagram. After this, the interband contributions to the experimental OC, σ_{inter}, were calculated as $\sigma_{inter}=\sigma_{exp}-\sigma_D$, where σ_{exp} is the experimentally determined OC and $\sigma_D=\Omega_P^2\gamma/4\pi(\omega^2+\gamma^2)$ is the Drude term. Then, a multiple-peak analysis using the symmetrical Gaussians was applied to the obtained σ_{inter} spectra. The decomposition results for σ_{inter}, together with the results of Ω_P and γ calculations, are presented in Table II and Fig. 5(c) (for $T=78$ K, as an example.)

It is seen that the interband OC spectrum for the ferromagnetic cubic Ni_2MnGa alloy ($T_{meas}=293$ K) has two interband absorption peaks at 1.78 (peak A) and 3.40 eV (peak B) (see Table II). Since no result of the first-principles calculation for the DF of the Ni_2MnGa alloy is available, for the further discussion we refer to the theoretical[15] and experimental[19] results obtained for the isostructural Ni_2MnSn alloy.

The optical properties of several ferromagnetic Heusler alloys containing Mn at the *Y* sites were theoretically examined by Kubo *et al.*[15–17] It was shown that the OC spectra for Cu_2MnAl, Pd_2MnSn, and Ni_2MnSn alloys are rather similar to each other and reveal a group of interband absorption peaks in the 1–4-eV energy range, which have the same nature. Furthermore, the experimental OC spectrum of Ni_2MnSn alloy in the 0.5–4.0 eV energy range[19] is in a fairly good agreement with theory and also looks very similar to our experimental OC spectra. Therefore, we can presumably apply the theoretical results obtained for the Ni_2MnSn alloy to the Ni_2MnGa alloy. According to Kubo *et al.*[17] a strong interband absorption occurs at ~ 0.3 eV, and sharp peaks appear at 2.0 and 3.4 eV. Broad peaks located at $\sim$ 5.0 and 7.2 eV were also mentioned. It was shown that the structure at 2 eV in the ε_2 spectrum is formed by the electronic excitations from the 13th and 14th bands to the 15th band (further designation is 13,14→15) in the minority-spin band, while the peak near 3.4 eV is formed by the (13,14→19) and (18,19→20) transitions in the minority- and majority-spin bands, respectively. Transitions (13→15) and (14→15) take place from regions around Γ, *L*, and *K* points near E_F in the Brillouin zone while, in formation of the other transitions, quite a large volume of Brillouin zone has to be taken into account. Here we must note that Kirillova *et al.* did not mention the low-energy peak at 0.3 eV, predicted by theory.[19]

The main cause for the temperature dependence of the electronic structure and hence the optical properties of nonmagnetic metals is a change of the lattice with temperature. In order to minimize the influence and obtain the results comprising the entire ferromagnetic→paramagnetic transition, we also studied the optical properties of the paramagnetic Ni_2MnGa alloy just above the Curie temperature, i.e., at $T/T_C=1.08$ (409 K). Disappearance of the ferromagnetic order turns out not to change significantly the interband OC spectrum of the Ni_2MnGa alloy (see Fig. 5 and Table II). This means, at least, that the initial and final states in the $E(\mathbf{k})$ spectra involved in formation of the interband peaks are not altered, or shifted in a parallel way. Nearly the same result was obtained for the bulk annealed sample measured at $T/T_C=1.21$ (not shown). The invariance of interband OC spectra for both ferromagnetic and paramagnetic phases of the Ni_2MnGa alloy looks unexpected in a view of Velikohatnyj and Naumov.[26] The calculated DOS for the ferromagnetic and paramagnetic states are significantly different.[17,26] Therefore, a certain difference in the joint density of states between paramagnetic and ferromagnetic phases is expected. At the same time, changes in the values of Ω_P and γ, caused by the ferromagnetic→paramagnetic transformation, take place (see Table II). The enhancement of γ for the paramagnetic phase can be easily explained by an increase in the electron-phonon contribution to the effective relaxation frequency with increasing temperature. Similar fitting results were demonstrated upon the martensitic transformation. The values of plasma and relaxation frequencies for the tetragonal phase are smaller than those for the cubic one (see Table II). The reduction in γ for the tetragonal phase is readily understood for the same reason as for the case of the ferromagnetic→paramagnetic transition, i.e., a decrease in the electron-phonon contribution to the effective relaxation frequency with decreasing temperature.

A caution is advised here. The numerical values of Ω_P and γ bear no significant physical meaning. The trend of change in γ has a certain physical meaning so that it follows a reasonable dependence on temperature. For Ω_P, however, at least three factors are involved; free-carrier density, effective mass, and screening or effects of interband absorption. Since clear information on each of these is not known, it is quite dangerous to give too much physical significance to the numerical values of Ω_P. In addition, one cannot absolutely

disregard the possibility of very low-energy interband absorption. Therefore, to be more safe, these numbers should be merely taken as fitting parameters for the analysis of OC spectra.

The nearly perfect resemblance observed in the interband OC spectra for the ferromagnetic and paramagnetic states can be understood in terms of the fluctuation theory for ferromagnets. According to such an approach, the disappearance of ferromagnetism is explained, for example, by breaking the magnet at T_C into randomly oriented dynamic regions or clusters, each of which maintains nearly the same magnetic order as in the ferromagnetic state. Because of the absence of ferromagnetic coupling between these clusters, the resultant (macroscopic) magnetization vanishes at T_C. According to Ref. 31 these dynamic regions, or spin correlations, exist for $t_{sc} \sim \hbar/T_C \sim 10^{-13}$ s. Because of the relatively large number of electrons involved in this process, t_{sc} is significantly longer than the time for formation of the electronic structure $\sim \hbar/W_d \sim 10^{-15}$s for a magnetic material, where W_d is the width of the d band. Therefore, the one-particle states within a dynamic magnetic cluster have enough time to be reconstructed according to the potential fields created by the "slow" spin-density fluctuations, and the local band structure in the region of the spin fluctuation is the same as that at $T=0$, while the magnetization directions of clusters are distributed randomly in space. Thus, photons cannot detect the difference between ferromagnetic and nonmagnetic states of alloy.

The structural transformation from cubic to tetragonal lattice leads to more noticeable changes in the interband absorption spectrum of the Ni_2MnGa alloy than for the case of the ferromagnetic→paramagnetic transition. Both interband absorption peaks are reduced in magnitude: peak A does not change its position in the OC spectrum, while peak B exhibits a redshift by about 0.2 eV (see Table II).

Comparing the DOS curves for the cubic and tetragonal phases, one can conclude that the difference between them is less noticeable than between cubic ferromagnetic and paramagnetic phases. However, experimentally the difference in the interband OC spectrum is reversed. Thus, it is clear that the first-principles calculations on the optical properties of the cubic and tetragonal phases of the Ni_2MnGa alloy should be employed for a better elucidation of the experimentally observed structural and temperature dependencies of the optical properties.

C. Magneto-optical properties of the alloy

Before carrying out the spectral EKE measurements the magnetic-field dependence of the MO response $\delta_p(H)$ should be known. Figure 6 shows the results of such a study at 293 K for a crystalline Ni_2MnGa alloy film (sample No. 4), together with the magnetization hysteresis loops $M(H)$ (in-plane geometry), measured at 293 K, for the bulk and film (sample No. 4) samples.

It is seen in Fig. 6 that the MO response nearly reaches the saturation at an ac magnetic field of 950 Oe, which is the maximum ac magnetic field available for our MO measurements, while the full saturation for the bulk and film samples

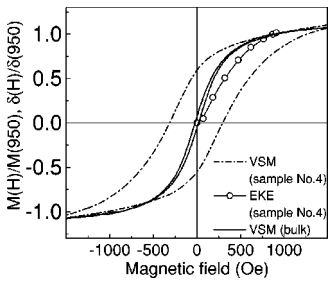

FIG. 6. Magnetization hysteresis loops for the bulk (solid line) and crystalline-film (sample No. 4) (dash-dotted line) Ni_2MnGa alloy samples. Open circles present the ac magnetic-field dependence of EKE responses for sample No. 4. All the measurements were carried out at 293 K.

is achieved at a field of ~1500 Oe according to the VSM measurements. A significant difference in coercivity for the bulk and the crystalline film is probably caused by different crystallite dimensions. Unlike the bulk and the crystalline film all the investigated amorphous alloy films (sample Nos. 2, 3, and sample No. 4 before annealing) are not ferromagnetically ordered at RT. However, annealing of such an amorphous film, which restores its crystalline structure, leads back to the ferromagnetic properties. A significant structural dependence of the magnetic properties of Heusler alloys is a well-known phenomenon. Ikeda and Takahashi[32] explained theoretically decreases in magnetization and Curie temperature for the cold-worked Mn-based Heusler alloys, induced by significantly different magnetic properties of the Mn atoms near the antiphase boundaries produced by a plastic deformation. Krusin-Elbaum *et al.*[33] reported that amorphous Cu_2MnSn exhibits a spin-glass behavior. On the other hand, Orgassa *et al.*[34] have shown that occupation by the atoms at the improper sites in the lattice, or atomic disordering for the semi-Heusler NiMnSb alloy, leads to a decrease in spin polarization, which explains the structural dependence of magnetic properties. Thus, the experimentally observed nonmagnetic properties of amorphous Ni_2MnGa are general for Heusler and semi-Heusler alloys, however, the detailed investigation of the magnetic properties is out of the scope of the present paper.

The EKE spectra for bulk and crystalline Ni_2MnGa alloy samples are shown in Fig. 7. All the experimentally observed EKE values were artificially saturated by using a scaling factor determined from the comparison of the $M(H)$ and the $\delta_p(H)$ dependencies. All these spectra look very similar to each other, exhibiting a strong negative peak at $\hbar\omega \approx 3$ eV and a noticeable positive peak at 1.25 eV. On the other hand, the amplitudes of EKE spectra are significantly different. For example, the EKE spectrum for alloy film No. 4, which has a worse crystallinity than film No. 1, exhibits the largest negative peak at about 3 eV among the investigated samples. Similar to the results of magnetic measurements by VSM, no MO response was detected at RT for all the investigated amorphous Ni_2MnGa alloy films.

In order to understand the reason for the noticeable difference in magnitude of the EKE spectra, the off-diagonal components of the DF were calculated using the correspond-

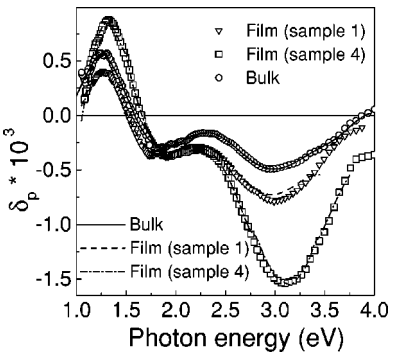

FIG. 7. Experimental EKE spectra for the bulk and crystalline-film (sample Nos. 1 and 4) Ni_2MnGa samples. Lines present EKE spectra for the corresponding samples, simulated with use of the experimentally determined diagonal and off-diagonal components of the DF.

ing optical data and the results of EKE measurements at two angles of incidence. The results are shown in Fig. 8. It is seen that all these spectra show a resemblance in the spectral shape and the peak position; the absorptive part of the off-diagonal components of the DF shows two pronounced negative peaks at 1.75 and 2.8 eV. The intensities of peaks in the $\varepsilon_2' \times (\hbar\omega)^2$ spectra are different for the samples, however, the same regularity in the dependence on crystallinity as for the optical properties is observed, i.e., the better the crystallinity of the sample, the larger the value of $\varepsilon_2' \times (\hbar\omega)^2$. The correctness of the determined off-diagonal components of the DF was checked by restoring the EKE spectra via a simulation procedure which uses ε_1, ε_2, ε_1', and ε_2' as input parameters. The results are shown by lines in Fig. 7. It is seen that there is no doubt regarding the correctness in determining the off-diagonal components.

Thus, we can conclude that the values of the diagonal and off-diagonal components of the DF in the interband absorption region are dependent strongly upon the crystallinity of alloy, showing a regularity; the better the crystallinity, the larger the values of the DF (at least, in the regions of interband absorption). The second conclusion is that the MO response depends significantly not only on their magnetic properties and spin-orbit interaction but also on their optical parameters. If the off-diagonal components of the DF are large, the MO response is, in general, also enhanced. However, the MO response is determined by not only the off-diagonal components but the diagonal ones. If the diagonal components are large, the MO response is reduced because the diagonal components enter into the denominator of the equation for the MO response. This is the reason why sample 4, which has the worst crystallinity, exhibits the largest EKE response (see Fig. 7). All the investigated samples have almost the same small magnitudes of ε_1 and thus the denominator is mainly determined by the magnitude of ε_2 or OC. Sample 4 has the smallest OC value in the interband absorption region (see Fig. 4), resulting in the largest MO response.

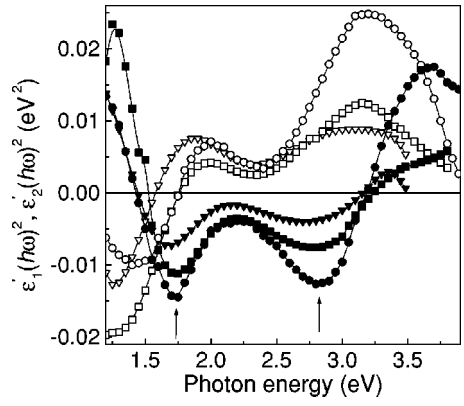

FIG. 8. $\varepsilon_1' \times (\hbar\omega)^2$ (open symbols) and $\varepsilon_2' \times (\hbar\omega)^2$ (solid symbols) spectra for the electropolished bulk (circles) and crystalline-film [sample Nos. 1 (squares) and 4 (down-triangles)] Ni_2 MnGa alloy, measured at 293 K. The spectra for the bulk sample are plotted with a scaling factor of 0.45.

The nature of the peaks in the absorptive part of the off-diagonal components of the DF, $\mathrm{Im}[\sigma_{xy}(\hbar\omega)]$, is best understood, if, in accordance with the results by Uspenski and Halilov,[35] $\mathrm{Im}[\sigma_{xy}(\hbar\omega)]$ is represented as a difference between the optical conductivities with opposite spins, i.e., $\mathrm{Im}[\sigma_{xy}(\hbar\omega)] \approx \alpha' \{\mathrm{Re}[\sigma_{xx}^{\uparrow}(\hbar\omega)] - \mathrm{Re}[\sigma_{xx}^{\downarrow}(\hbar\omega)]\}$. The condition for this approximation is fulfilled when $2\xi \ll \hbar\omega < W_d$, where ξ is the spin-orbit interaction strength [$\xi \equiv (1/2m^2c^2)(1/r(dV/dr)]$ and W_d is the d-band width. The spin-orbit interation strength is usually an order of 10 meV and the d-band width for Mn and Ni is about 5–6 eV. Therefore, we can apply the above approximation for our measured energy range. As aforementioned, the low-energy interband absorption peak (peak A) in the OC spectrum of the alloy is formed mainly by the electron transitions in the minority-spin subbands. Thus, because the $\sigma_{xx}^{\uparrow}(\hbar\omega)$ contributions to peak A is negligible, the spectrum of the absorptive part of the off-diagonal components of the DF should contain a peak at the same energy as in the OC spectrum. It is seen that the low-energy peak in the $\varepsilon_2' \times (\hbar\omega)^2$ spectra is located exactly at the same energy as that in the OC spectra (see Figs. 5 and 8, and also Table II). This fact can be considered as other evidence that the presumed nature of the low-energy peak in the OC spectrum of the alloy is correct. At the same time, the electron transitions in both spin subbands contribute nearly equally to the formation of peak B in the OC spectrum. Therefore, their difference may produce a peak of complicated shape in the $\varepsilon_2' \times (\hbar\omega)^2$ spectra and hence the high-energy peak in the $\varepsilon_2' \times (\hbar\omega)^2$ spectra is observed at a different energy from that in the OC spectra.

IV. SUMMARY

(i) The optical and MO properties of the Ni_2MnGa alloy were investigated for the martensitic and austenitic phases as well as for the ferromagnetic and paramagnetic states of the austenitic phase. The parameters of charge carriers, such as plasma and relaxation frequencies, were determined for all the mentioned states.

(ii) The interband OC spectrum in the 0–4-eV energy range for the ferromagnetic cubic phase of the Ni_2MnGa alloy exhibits two intense peaks at 1.78 and 3.40 eV. By the analogy with the Ni_2MnSn alloy the nature of these peaks is

discussed in terms of the band structure.

(iii) It was shown that the ferromagnetic-paramagnetic phase transformation in the Ni_2MnGa alloy changes the interband OC spectrum very insignificantly. This experimental result does not support the theoretical predictions. An explanation of the disagreement between theory and experiment is suggested, based on the fluctuation theory of ferromagnets.

(iv) In contrast to the ferromagnetic-paramagnetic phase transformation, the transition to the martensitic phase causes more significant changes in the interband OC spectrum: the intensities of peaks become smaller, and the low-energy peak retains its location while the high-energy peak exhibits a redshift by about 0.2 eV.

(v) The film deposition onto substrates cooled by liquid nitrogen leads to the formation of a substantially disordered or amorphous phase in the Ni_2MnGa alloy, which is not ferromagnetically ordered at RT. Annealing of the amorphous films at 680 K for 60 min restores their crystallinity and also the ferromagnetic order.

(vi) The off-diagonal components of the DF for the cubic phase of the Ni_2MnGa alloy was determined. As in the interband OC spectrum, the absorptive part of the off-diagonal components of the DF exhibits a two-peak structure, in which the low-energy peak is located at the same energy as that in the OC spectrum. Both optical and MO properties of the Ni_2MnGa alloy show a noticeable structural dependence; the better the crystallinity of the sample, the larger the intensities of peaks in the interband absorption region.

(vii) It was shown that the MO response for the Ni_2MnGa alloy is strongly influenced by the optical properties and should be considered to have a close connection with them.

ACKNOWLEDGMENTS

This work was supported by the KOSEF through the Quantum Photonic Science Research Center, and by Korea Research Foundation Grants (No. KRF-2001-015-DS0015 and KRF-01-DP0193). We are also grateful to J. Dubowik for the help with the magnetic measurements and to Y. N. Petrov for the TEM study of film samples.

[1] P.G. van Engen, K.H.J. Buschow, R. Jongebreur, and M. Erman, Appl. Phys. Lett. **42**, 202 (1983).
[2] P.A.M. van der Heide, W. Baelde, R.A. de Groot, A.R. de Vroomen, P.G. van Engen, and K.H.J. Buschow, J. Phys. F: Met. Phys. **15**, L75 (1985).
[3] R. Ohyama, T. Koyanagi, and K. Matsubara, J. Appl. Phys. **61**, 2347 (1987).
[4] M. Naoe, N. Kitamura, M. Shoji, and A. Nagai, J. Appl. Phys. **63**, 3636 (1998).
[5] S.V. Halilov and E.T. Kulatov, J. Phys.: Condens. Matter **3**, 6363 (1991).
[6] H. Fu, Z. Yan, S.K. Lee, and M. Mansuripur, J. Appl. Phys. **78**, 4076 (1995).
[7] E. Kulatov, Yu. Uspenskii, and S. Halilov, J. Magn. Magn. Mater. **145**, 395 (1995).
[8] J.F. Bobo, P.R. Johnson, M. Kautzky, F.B. Mancoff, E. Tuncel, R.L. White, and B.M. Clemens, J. Appl. Phys. **81**, 4164 (1997).
[9] V.N. Antonov, P.M. Oppeneer, A.N. Yaresko, A.Ya. Perlov, and T. Kraft, Phys. Rev. B **56**, 13 012 (1997).
[10] J. Pierre, R.V. Skolozdra, J. Tobola, S. Kaprzyk, C. Hordequin, M.A. Koiacou, I. Karla, R. Currat, and E. Lelièvre-Berna, J. Alloys Compd. **262-263**, 101 (1997).
[11] J.A. Caballero, W.J. Geerts, F. Petroff, J.-U. Thiele, D. Weller, and J.R. Childress, J. Magn. Magn. Mater. **177-181**, 1229 (1998).
[12] X. Gao, J.A. Woollam, R.D. Kirby, D.J. Sellmyer, C.T. Tanaka, J. Nowak, and J.S. Moodera, Phys. Rev. B **59**, 9965 (1999).
[13] V.N. Antonov, A.N. Yaresko, A.Ya. Perlov, V.V. Nemoshkalenko, P.M. Oppeneer, and H. Eschrig, Low Temp. Phys. **25**, 387 (1999).
[14] J. Tobola and J. Pierre, J. Alloys Compd. **296**, 243 (2000).
[15] Y. Kubo, S. Ishida, and J. Ishida, J. Phys. F: Met. Phys. **11**, 2443 (1981).
[16] S. Ishida, S. Akazawa, Y. Kubo, and J. Ishida, J. Phys. F: Met. Phys. **12**, 1111 (1982).
[17] Y. Kubo, N. Takakura, and S. Ishida, J. Phys. F: Met. Phys. **13**, 161 (1983).
[18] E.I. Shreder, M.M. Kirillova, and V.P. Dyakina, Phys. Met. Metallogr. **81**, 406 (1996).
[19] M.M. Kirillova, Yu.I. Kuz'min, Yu.V. Knyazev, and E.I. Shreder, Phys. Met. Metallogr. **83**, 590 (1997).
[20] J. van Ek, W. Huang, and J.M. MacLaren, J. Appl. Phys. **81**, 5429 (1997).
[21] E.I. Shreder, M.M. Kirillova, and V.P. Dyakina, Phys. Met. Metallogr. **90**, 362 (2000).
[22] V.V. Martynov and V.V. Kokorin, J. Phys. III **2**, 739 (1992).
[23] K. Ullakko, J.K. Huang, C. Kantner, and R.C. O'Handley, Appl. Phys. Lett. **69**, 1966 (1996).
[24] F.X. Hu, B.G. Shen, J.R. Sun, and G.H. Wu, Phys. Rev. B **64**, 132412 (2001).
[25] M. Pugaczowa-Michalska, Acta Phys. Pol. A **96**, 467 (1999).
[26] O.I. Velikohatnyj and I.I. Naumov, Phys. Solid State **41**, 617 (1999).
[27] Y.P. Lee, R. Gontarz, and Y.V. Kudryavtsev, Phys. Rev. B **63**, 144402 (2001).
[28] F. Zuo, X. Su, and K.H. Wu, Phys. Rev. B **58**, 11 127 (1998).
[29] A.N. Vasil'ev, A.D. Bozhko, V.V. Khovailo, I.E. Dikshtein, V.G. Shavrov, V.D. Buchelnikov, M. Matsumoto, S. Suzuki, T. Takagi, and J. Tani, Phys. Rev. B **59**, 1113 (1999).
[30] S. Wirth, A. Leithe-Jasper, A.N. Vasil'ev, and J.M.D. Coey, J. Magn. Magn. Mater. **167**, L7 (1997).
[31] *The Dynamical and Kinetic Properties of Magnets*, edited by S.V. Vonsovsky and E.A. Turov (Science, Moscow, 1986), p. 12.
[32] K. Ikeda and S. Takahashi, Phys. Rev. B **30**, 3808 (1984).
[33] L. Krusin-Elbaum, A.P. Malozemoff, and R.C. Taylor, Phys. Rev. B **27**, 562 (1983).
[34] D. Orgassa, H. Fujiwara, T.C. Schulthess, and W.H. Butler, Phys. Rev. B **60**, 13 237 (1999).
[35] Y.A. Uspenski and S.V. Halilov, Zh. Éksp. Teor. Fiz. **95**, 1022 (1989) [Sov. Phys. JETP **68**, 588 (1989)].